

Polarization and Relaxation Processes in He³ Gas*

RODGER L. GAMBLIN† AND THOMAS R. CARVER

Palmer Physical Laboratory, Princeton University, Princeton, New Jersey

(Received 16 October 1964; revised manuscript received 7 January 1965)

Polarization of He³ when used as a buffer gas for optically pumped rubidium vapor has been investigated experimentally and theoretically. Experiment shows that the coupling between a rubidium and He³ atom is scalar in form (i.e., $\mathbf{I}\cdot\mathbf{S}$) and is about three orders of magnitude greater than would be expected from the direct magnetic interaction of the dipoles associated with each atom. A theoretical explanation of this effect, which depends upon the overlap of the Rb valence electron with the electrons of the He³ atom is presented and is in agreement with experiment. Experiments concerning the optical pumping of metastable He³ atoms in order to produce ground-state polarization are described. Polarizations of 60% in 1-Torr (1 STP mm) samples at room temperature and 56% in 3-Torr samples at 77°K have been achieved. The process of metastable pumping works only at these lower pressures. Mercury liquid is shown experimentally, however, to present a poor surface for He³ relaxation. This result opens the possibility of achieving high polarization at high pressure using metastable pumping and gas compression. Various wall coatings of He³ samples are found to have only small effects upon relaxation rates. A 3.1-amagat (1 STP atm) sample in Pyrex but of high purity is found to have a relaxation time of 2×10^4 sec. This value sets present limits upon the experimental He³-He³ relaxation cross section. A new effect which involves relaxation processes of the He³ polarization in a magnetic field with a gradient is investigated both experimentally and theoretically. The results of both theory and experiment are in close agreement with each other. An effect involving enhanced polarization of either sign of spin temperature of a high-pressure sample of He³ in which a gas discharge is struck, and which is in a 10-kG field, is described experimentally.

INTRODUCTION

General

PERHAPS the greatest motivation for research with He³ polarization is the desirability of performing nuclear-physics and elementary-particle experiments upon oriented nuclei. This object has led to considerable work in the past in order to find a mechanism to polarize a few-cc sample of at least an amagat (1 STP atm) density to a level of 50% or greater.

Polarization of He³ by brute force is virtually impossible. In a 123-G field at room temperature the relative polarization is 3.4×10^{-8} . By cooling the sample to 0.03°K, one could gain a factor of 10^4 so that one would have a 3.4×10^{-4} polarization if exchange effects are neglected. In this case one would need a field of 147 kG. Both the temperature and field, but especially the latter, would be extremely difficult to achieve. Since He³ is a Fermi-Dirac liquid at low temperatures, the Curie susceptibility is no longer valid, and the problem is intensified. One is thus led to consider various forms of dynamic polarization which have the advantage of operating at reasonable fields and temperatures.

The following paper describes experimental and theoretical results obtained in attempting to polarize He³ and in the related problem of He³ relaxation.

Rubidium Optical Pumping

In 1960 Bouchiat, Carver, and Varnum¹ reported an enhancement of approximately 10^4 in polarization in

* Research supported by the National Science Foundation.

† Submitted in partial fulfillment of the requirement for the degree of Doctor of Philosophy to the Department of Physics at Princeton University. Present address: IBM General Products Division Development Laboratory, Endicott, New York.

¹ M. A. Bouchiat, T. R. Carver, and C. M. Varnum, *Phys. Rev. Letters* **5**, 373 (1960).

a 2.1-amagat sample of He³ over its equilibrium value at room temperature in a 123-G field. The method was to optically pump rubidium vapor with a buffer gas of He³. In their work they assumed that dipolar coupling between the Rb and He³ spin systems led to the results. Subsequent work, which is reported below, has shown that the interaction between the Rb and He³ spin systems is scalar (i.e., $\mathbf{I}\cdot\mathbf{S}$) in form and enhanced by about a factor of 10^3 over the scalar part of the dipolar interaction. As will be discussed in more detail, it appears that optical pumping on Rb to polarize He³ at high pressures is unlikely to achieve degrees of polarization of more than a few tenths of a percent. These levels are too low to be of use in high-energy physics; however, in the course of the work with the Rb-He³ system, it became clear that the mechanism of coupling between the two atoms in a collision is considerably different from the previous theoretical prediction. In collisions between atoms such as Rb and He³, Abragam² predicted that the interaction between the electronic and nuclear dipoles would lead to a predominance of operators of the form I_+S_+ or I_-S_- , where I_{\pm} and S_{\pm} are the angular-momentum raising and lowering operators for the nuclear and electron spins. Abragam's calculations are based on the rather appealing model of direct magnetic interaction between the dipoles of the two atoms. The magnitude of such an interaction yields a cross section of the order of 10^{-27} cm² for a spin-flip process. The experimental work of this paper shows, however, that the cross section of interaction between Rb and He³ is more on the order of 10^{-24} cm² and that it is scalar in form. By scalar is meant an interaction of the form $\mathbf{I}\cdot\mathbf{S}$ which leads to spin-flip operators of I_+S_- or I_-S_+ . A theoretical explanation of this interaction is developed

² A. Abragam, *Phys. Rev.* **90**, 1729 (1955).

in this paper and depends upon overlap or interference effects between the valence electron of the Rb atom and the electrons of the He³ atom. Experiment and theory are in reasonable accord.

He³ Relaxation

In this paper two rather contrasting subjects concerning He³ relaxation will be discussed. One will be a relaxation mechanism when a sample of polarized gas is in a magnetic field with a gradient. With the theory presented below, the mechanism is well understood. The second subject will concern relaxation of He³ in a homogeneous field. As yet there seems to be no theory to cover experimental results in this area.

The dipolar interaction between He³ nuclei can cause relaxation of polarization but is an extremely weak effect. The mechanism for relaxation arises through operators of the form $I_{\pm}S_{\pm}$ or $I_{\pm}S_z$ in the dipole interaction. An easy estimate of the time for polarization decay can be arrived at by noting that the time of interaction is of the order of an atomic diameter divided by the velocity. This time is short compared to the inverse of the frequency change in a transition so that, in the spirit of time-dependent perturbation theory, one can approximate the probability of transition as the square of the energy of interaction times the number of collisions per second. Since the collisions are not correlated, this quantity yields the inverse of T_1 , i.e.,

$$1/T_1 = \gamma^4 \hbar^2 n / v^2 d^4, \quad (1)$$

where n is the number of collisions per second, d is the atomic diameter, and v^2 is the mean-squared velocity. This formula yields $T_1 \approx 10^6$ sec for He³ at 3 amagats. Experimental results are presented subsequently that indicate that 3-amagat samples can be made which have relaxation times as long as 2.3×10^4 sec. This number is, however, the maximum T_1 of a number of samples all of which have relaxation times varying at random over an order of magnitude. Since the relaxation time seems to be independent of various nonmagnetic wall materials, one can perhaps only guess at the mechanism of relaxation as being adsorbed impurities on the wall surfaces. Experimental evidence to support this view is presented below.

A controllable mechanism of relaxation in gases arises when samples are in inhomogeneous fields, as reported by Gamblin and Carver.³ If an atom is in a field with a gradient, its thermal motion causes it to experience a time-varying component of the field. As an atom moves between collisions, the magnetic moment of the atom tends to become disaligned from the field. If one gets in a frame of reference in the moving frame of the particle such that the magnetic field maintains its orientation along the z axis, then the atom "sees" a static perpendicular component of field in this frame. It then, in

this frame, precesses about the resultant field. When the atom makes a collision with another, its direction of motion changes. In the atom's own frame of reference, the effective static component of field that it sees thus suddenly shifts to a new direction. The atom then begins to precess about this new effective field. The amount of disorientation in each flight can be viewed as a step in a random walk as will be shown below. As the atom makes many collisions, the magnetic moment becomes disoriented from the field direction. In gases this effect is surprisingly large. Relaxation times for the process are, in all but the higher pressures and more homogeneous fields, shorter than obtainable spin-lattice relaxations in clean samples of He³. Colegrove, Scheerer, and Walters⁴ and Kleppner, Goldenberg, and Ramsey⁵ have also observed relaxation in inhomogeneous fields.

Optical Pumping of Metastable He³

If one takes a pure sample of He³ at a density on the order of 1 Torr (1 STP mm) and strikes a weak electrical discharge in it, ³S₁ metastable atoms are formed. One thus has a mixture of two types of atoms in the sample, those in the ground state and metastables. The metastable atoms have an energy configuration suitable for optical pumping. If one uses circularly polarized light from a He⁴ lamp, the ³S₁ → ³P₀ metastable transition is primarily illuminated. Angular momentum is absorbed by the metastables and their nuclei become polarized. Metastables in a collision with a neutral atom have a large cross section (10^{-16} cm²) for exchange of metastability. In these collisions the nucleus is, however, unaffected by the exchange so that if one has a metastable with a polarized nucleus in collision with a neutral with a disoriented nucleus, the result of the collision will be a polarized neutral and a depolarized metastable which can then be optically pumped to the oriented state. The polarization of the nuclei of the metastables is thus tightly coupled to the polarization of the ground state. Optical pumping on the metastables serves to orient the ground state.

High degrees (60%) of polarization have been achieved by this method, but in samples of the order of a millimeter in pressure. At present, if a means could be found to increase the pressure of a sample of gas, high polarization at high pressure might be achieved. Since, as will be discussed later, a clean mercury surface does not appear to relax oriented He³ nuclei at a rate faster than Pyrex, a large container could be illuminated and a mercury surface used to compress the resulting polarized gas to a small volume at high pressure.

Phelps and Molnar⁶ and Phelps⁷ have investigated the destruction of ³S₁ helium atoms and found that at

⁴ F. D. Colegrove, L. D. Scheerer, and G. K. Walters, *Phys. Rev.* **132**, 2561 (1963).

⁵ D. Kleppner, H. M. Goldenberg, and N. F. Ramsey, *Phys. Rev.* **116**, 603 (1962).

⁶ A. V. Phelps and J. V. Molnar, *Phys. Rev.* **89**, 1202 (1953).

⁷ A. V. Phelps, *Phys. Rev.* **99**, 1307 (1955).

³ R. L. Gamblin and T. R. Carver, *Bull. Am. Phys. Soc.* **2**, 11 (1964).

low densities of metastables, the mechanism of decay at high helium pressures is through the formation of three-atom metastable molecules in three-body collisions. At low helium pressures, diffusion to the walls dominates the decay. Since the cross section for the three-body process is a rapidly varying function of temperature, optical pumping at 77°K could possibly allow greater degrees of polarization. This effect was observed, but the percentage polarizations at higher pressures (10–30 mm) are less than 20%. This result would lead one to believe that the metastable concentration is high enough so that metastable-metastable collisions limit the density of metastables. The ultimate polarization would then be a function of the input light intensity and the relaxation time under discharge conditions. Colegrove, Scheerer, and Walters⁴ in their discovery and subsequent investigation of the metastable polarization mechanism have, in general, reported lower polarizations than those given below.

Intermittent Discharge Effects

If an intermittent spark discharge of high frequency is created in a clean sample of three-amagat He³ which is maintained in a 10-kG field, some interesting effects arise. The nuclear magnetism is enhanced by about a factor of 4. The spin temperature is negative, however. The spins align against the field. If the discharge is made continuous, on the other hand, the same enhancement-amplitude increase is observed, but the spin temperature is positive.

The explanation of this strange behavior is, tentatively, that the existence of a predominance of saturated metastables or molecules in the intermittent case leads to an Overhauser-type effect which tends to align spins against the field. In the continuous case, saturated electrons could lead to an alignment with the field through dipolar coupling.

CALCULATIONS

Rubidium-He³ Interaction

As was pointed out in the introduction, overlap effects influence the interaction between the Rb valence electron and the He³ nucleus. The approach used below will be to let the dipolar energy operator act in time-dependent perturbation theory between the two spin orientations of the He³ nucleus with the initial spin direction of the Rb atom assumed given. The ground-state wave functions will be written in an orthogonal form, however, and as will be seen, the matrix element formed with these functions contains terms which describe the hyperfine-contact-interaction enhancement.

Let the wave function of the Rb electron be ψ , where ψ represents both a space and spin function. Let the Rb valence electronic function of opposite spin be ϕ . Let α_1, β_1 and α_2, β_2 be the electronic wave functions for the He³ atom with the subscript referring to the identity of

the particles and α and β referring to the two possible spin states, with α having the same spin orientation as ψ . A suitable orthonormal set of functions formed from these functions is

$$\begin{aligned}\alpha_1' &= \alpha_1, \\ \beta_2' &= \beta_2, \\ \beta_1' &= \beta_1 - \langle \beta_1 | \beta_2 \rangle \beta_2, \\ \alpha_2' &= \alpha_1 - \langle \alpha_1 | \alpha_2 \rangle \alpha_2, \\ \psi' &= (\psi - \langle \psi | \alpha_1 \rangle \alpha_1) / (1 - \langle \psi | \alpha_1 \rangle^2)^{1/2}, \\ \phi' &= (\phi - \langle \phi | \beta_2 \rangle \beta_2) / (1 - \langle \phi | \beta_2 \rangle^2)^{1/2}.\end{aligned}\quad (2)$$

The energy of interaction between an electronic spin of index μ and a nucleus of index α is

$$\mathcal{H}_{\alpha\mu} = \frac{2\beta\mu_\alpha}{I_\alpha} \left(\frac{8\pi}{3} \mathbf{I}_\alpha \cdot \mathbf{S}_\mu \delta(\mathbf{r}_\mu - \mathbf{r}_\alpha) + \frac{3\mathbf{S}_\mu \cdot (\mathbf{r}_\mu - \mathbf{r}_\alpha) \mathbf{I}_\alpha \cdot (\mathbf{r}_\mu - \mathbf{r}_\alpha)}{|\mathbf{r}_\mu - \mathbf{r}_\alpha|^5} - \frac{\mathbf{S}_\mu \cdot \mathbf{I}_\alpha}{|\mathbf{r}_\mu - \mathbf{r}_\alpha|^3} \right). \quad (3)$$

\mathbf{I}_α and \mathbf{S}_μ are, respectively, the nuclear and electronic spin vectors, β is the Bohr magneton, μ_α is the nuclear moment, and I_α the nuclear spin. Without overlap enhancement this energy of interaction leads to a cross section of spin exchange on the order of 10^{-27} cm², as shown, for example, by Herman.⁵ The ratio of the overlap terms for the δ function part of (3) to the last two terms is given roughly by

$$\frac{\int \psi(\mathbf{r}_\mu) \alpha(\mathbf{r}_\alpha) \delta(\mathbf{r}_\mu - \mathbf{r}_\alpha) d\mathbf{r}_\mu}{\int \psi(\mathbf{r}_\mu) \alpha(\mathbf{r}_\alpha) |\mathbf{r}_\mu - \mathbf{r}_\alpha|^{-3} d\mathbf{r}_\mu}. \quad (4)$$

For helium, whose wave functions are approximated by hydrogen 1s functions with $z = 27/16$, (4) becomes very roughly $(a_0/zR)^3$, where R is the internuclear distance of the He³ and Rb atoms. The value of (4) thus is a number much less than 1. Subsequently only the first term of the interaction represented by (3) will be used. Writing the relevant parts of (3) in terms of spin-flip operators we have:

$$\mathcal{H} = \sum_i (8\pi/6) (\mu_i \mu_n) (I_+ S_{i-} + I_- S_{i+}) \delta(\mathbf{r}_i - \mathbf{r}_n), \quad (5)$$

where i refers to the electronic wave functions ψ, α , and β_2 . The only matrix element of $\langle \phi' | \mathcal{H} | \psi' \rangle$ which is nonzero is

$$\begin{aligned}M &= \left(\frac{8\pi}{6} \mu_n \mu_e (|\psi(B)|^2 - 2\langle \psi | \alpha \rangle |\alpha(0)| |\psi(B)| \right. \\ &\quad \left. + |\psi(B)|^2 \langle \psi | \alpha \rangle^2 |\alpha(0)|^2 \right) / (1 - \langle \psi | \alpha \rangle^2) \\ &= \frac{8\pi \mu_n \mu_e |\psi(B)|^2}{6(1 - \langle \psi | \alpha \rangle^2)} \left(1 - \frac{\langle \psi | \alpha \rangle |\alpha(0)|}{|\psi(B)|} \right)^2.\end{aligned}\quad (6)$$

⁵ R. M. Herman, Space Technology Laboratory Report 9820-6001-Ru-000 (Redondo Beach, California), 1964 (unpublished).

$\psi(B)$ is the probability amplitude of the Rb valence electron at the He³ nucleus. Using the Rb wave function of Callaway and Morgan⁹ but normalizing to 4π , and the hydrogen 1s wave function with $z=(27/16)$ for helium, then one can compute the above function. The Rb electronic wave function is assumed constant over the He³ atom since the He³ atom is much smaller than the extent of the Rb 5s electron. We find

$$\langle \psi | \alpha \rangle^2 \ll 1$$

$$M = (8\pi/6)\mu_n\mu_e |\psi(B)|^2 (-7)^2. \quad (7)$$

A large enhancement of the contact interaction thus exists because of electronic overlap effects. In a collision between the Rb and He³ atoms there is some effective distance of closest approach. Unless there exists a means for determining the potential function between the two atoms, there seems to be no good criteria for selecting any one particular value. The total cross sections for scattering of Rothe and Bernstein¹⁰ unfortunately yield primarily numbers for the Van der Waals attractive potential. The ionic crystal radii of Pauling¹¹ are probably too large because of the balancing out of attractive forces in a crystal, and gas kinetic cross sections, even if known, might more reflect the effects of the attractive force. One is thus left to select the distance of closest approach as a parameter of the theory as $3.4a_0$. The cross section is selected with a radius of $4.0a_0$. The physical process during a collision is that the helium atom penetrates the valence electron of the Rb atom and continues until it is stopped and reflected by the ionic core. If one considers a constant velocity during the process, then one can integrate $|\psi(B)|^2$ over a path numerically to and away from the point of closest approach. This process is equivalent to a time-dependent perturbation approach since the time of a collision is much shorter than the inverse of any energy difference times \hbar , for reasonable laboratory fields. Thus the cross section for spin flip is

$$\sigma_{\text{flip}} = \sigma_{\text{kinetic}} \left| (1/\hbar) \int M dt \right|^2. \quad (8)$$

The calculated cross section is 1.7×10^{-24} cm². There is an enhancement in the contact part of the dipolar interaction of 2.4×10^3 , so that in this case overlap effects are seen to have considerable importance. From an analysis of data given below, the experimental value of the cross section is shown to be 1.20×10^{-24} . The experimental coupling is also scalar which would not be the case if straight dipolar coupling with no electron overlap enhancement were present. Herman has pointed out the importance of overlap effects in rubidium-He³ collisions

⁹ J. Callaway and D. F. Morgan, Jr., Phys. Rev. **112**, 334 (1958).
¹⁰ W. Rothe and R. B. Bernstein, J. Chem. Phys. **31**, 1619 (1959).

¹¹ L. Pauling, *Nature of the Chemical Bond* (Cornell University Press, Ithaca, New York, 1940).

and has previously calculated the above cross sections.⁸

The selection of the distance of closest approach as $3.4a_0$ and the cross section as $\pi(4.0a_0)^2$ can be compared to taking the length parameter as the sum of Pauling's crystal radius of the Rb ion and the gas kinetic radius of the He³ atom. This value is $4.39a_0$. If one computes a cross section for the scalar spin-flip process using this value for both the distance of closest approach and the kinetic cross section one obtains 0.66×10^{-27} cm² which is within a factor of 2 of the observed value.

Wannier,¹² Löwdin,¹³ and Gourary and Adrian¹⁴ have discussed overlap effects and pointed out their importance in atomic interactions.

Overhauser Effects

A considerable amount of work has been done on various manifestations of the Overhauser effect, and an extensive literature has developed. A few key references are listed below.¹⁵⁻¹⁸ A more general name for the processes involved with the Overhauser effect that seems to be in common use is "dynamic polarization." Since all of the processes used for polarization in this paper depend upon the principle of the Overhauser effect, it seems reasonable to engage in a brief discussion of the principles involved.

If one has a set of states for a particular atom A , such as rubidium, or metastable He³, or an electron, each with a density in a sample of ρ_i and if W_{ij} is the probability of transition from state i to state j then, by detailed balancing, in equilibrium one has

$$\rho_i W_{ij} = W \rho_{av} \quad (9)$$

and

$$W_{ij} = W \exp(-\epsilon_i/kT). \quad (10)$$

Now, if one considers that the spin state of He³ atom is labeled with a "+" or "-", and if this state is coupled with one of the above states, one can use the symbol of W_{+-ij} to mean the transition probability of state i to j and + to -. In line with Eq. (9), then, in thermal equilibrium

$$W_{+-ij} = W \exp(-\epsilon_i/kT) \exp(-\delta/kT)$$

$$W_{-ji} = W \exp(-\epsilon_j/kT) \exp(\delta/kT), \quad (11)$$

where δ is the energy of the He³ nucleus in the magnetic field.

In a collision of a He³ atom upon atom A , spin-flip operators of the form $(I_+S_- + I_-S_+)$, $(I_-S_- + I_+S_+)$, or $(I_+S_z + I_-S_z)$ arise from some form of dipolar or scalar coupling, depending upon the nature of a collision. Furthermore, the same He³ atom in its flights between

¹² G. H. Wannier, Phys. Rev. **52**, 191 (1937).

¹³ Per-Olav Löwdin, J. Chem. Phys. **18**, 365 (1956).

¹⁴ R. S. Gourary and F. J. Adrian, Phys. Rev. **105**, 1180 (1957).

¹⁵ A. W. Overhauser, Phys. Rev. **92**, 411 (1953).

¹⁶ A. Abragam, Phys. Rev. **98**, 1729 (1955).

¹⁷ T. R. Carver and C. P. Slichter, Phys. Rev. **102**, 975 (1956).

¹⁸ R. H. Webb, Am. J. Phys. **29**, 428 (1961).

collisions tends to have its spin flipped by agents external to effects of atom A .

If one now wishes to compute the probability of spin flip per atom of He^3 in a particular state then one must consider the probability of spin flip due to collisions with each of the states i of atom A , plus the probability of flips due to external agents. If one labels each of the operators which act between the He^3 and A atoms with amplitudes a , b , and c and these numbers include the strength of interaction, a velocity, and an effective kinetic cross section, then the probability of a spin flip of a He^3 atom due to the atoms in state i is

$$W_{i+} = \sum \rho_i (a^2 \langle \psi_{j-} | I_- S_+ | \psi_{i+} \rangle^2 + b^2 \langle \psi_{j-} | I_- S_- | \psi_{i+} \rangle^2 + c^2 \langle \psi_{j-} | I_- S_z | \psi_{i+} \rangle^2) \times \exp(-\epsilon_i/kT) \exp(\delta/kT). \quad (12)$$

Then the sum of W_i over i is the probability of a transition for He^3 atom due to atom A . The probability of transition due to external agents can be represented by (n/τ) , where n is the number of He^3 atoms per cm^3 and τ is a time constant. The energy level represented by δ is about three orders of magnitude smaller than the ϵ_i so that $\exp(\pm\delta/kT)$, for most work, can be taken as unity. The difference in density between the two states of the He^3 atom in equilibrium will be given as unity because of this neglect.

Consider the Rb^{87} atom as atom A . In its ground state, it has $F=2$ and $F=1$ states; thus since

$$\begin{aligned} \sum_{m_F'} \langle 2, m_F' | S_+ | 2, m_F \rangle^2 &= (F - m_F)/2F, \\ \sum_{m_F'} \langle 2, m_F' | S_- | 2, m_F \rangle^2 &= (F + m_F)/2F, \\ \sum_{m_F'} \langle 1, m_F' | S_+ | 1, m_F \rangle^2 &= (F + m_F)/2F, \\ \sum_{m_F'} \langle 1, m_F' | S_- | 1, m_F \rangle^2 &= (F - m_F)/2F, \end{aligned} \quad (13)$$

one can, after a considerable simplification, write

$$\begin{aligned} dn/dt &= \sum_{F, m_F} \rho_{F, m_F} (a^2 + b^2 + 2c^2) n e^{\epsilon_{F, m_F}/kT} \\ &+ \sum_{m_F} \rho_{2, m_F} (m_F/2) (a^2 - b^2) n_0 e^{-\epsilon_{2, m_F}/kT} \\ &- \sum_{m_F} \rho_{1, m_F} m (a^2 - b^2) n_0 e^{-\epsilon_{1, m_F}/kT}, \end{aligned} \quad (14)$$

where n is the net polarization of the He^3 and n_0 is the He^3 density in atoms/ cm^3 . From Eq. (14) it can be seen that one must have a non-equilibrium value for the ρ_{F, m_F} and a predominance of either $I \pm S \mp$ or $I \pm S \pm$ coupling for enhancement to occur. If one can determine the ρ_{F, m_F} and the sign of n then one can determine the sign of $(a^2 - b^2)$ which in turn gives the form of the interaction between the Rb and He^3 atoms. This procedure is used below. Equation (14) can be further simplified by allowing the first sum to equal the Rb density, N . If one includes the external relaxation then

$$\begin{aligned} dn/dt &= -N_n \sigma' v - (2n/\tau) \\ &+ \sum_{m_F} \rho_{1, m_F} (m_F/2) (a^2 - b^2) n_0 \exp(-\epsilon_{2, m_F}/kT) \\ &- \sum_{m_F} \rho_{1, m_F} (m_F) (a^2 - b^2) n_0 \exp(-\epsilon_{1, m_F}/kT), \end{aligned} \quad (15)$$

where $\sigma' v = a^2 + b^2 + 2c^2$.

If, as can be determined from the relative orientation of the nuclear and electronic spin orientations, the coupling is scalar, and if experimental conditions are selected so that $\rho_{2,2} \gg \rho_{2, m_F=2}$ and $\rho_{2,2} \gg \rho_{1, m_F}$, and since $(1/\tau) \gg N\sigma v$, then in steady state

$$\sigma v = a^2 = 2n/(n_0 N \tau), \quad (16)$$

and one can compute the experimental cross section, for the Rb-He^3 interaction.

Inhomogeneous Fields Relaxation

As was pointed out in the introduction, when a sample of nuclear spins is placed in a magnetic field which is inhomogeneous, a much lessened T_1 may result. The effect arises because the spins, undergoing thermal motion in a nonuniform field, experience a time variation of field in their own frame of reference.

In order to gain physical insight into the mechanism of inhomogeneous field relaxation, consider a magnetic moment in and aligned with a static field. If the static field starts to rotate, one can get in a frame of reference such that the field maintains its orientation along the z axis. In this frame, as discussed, for example, by Slichter,¹⁹ the magnetic moment sees an additional component of field in the direction of rotation so that the total field will be

$$\mathbf{H}_{\text{tot}} = \mathbf{H}_0 + \mathbf{H}_{\text{eff}}; \quad \mathbf{H}_{\text{eff}} = -\mathbf{\Omega}/\gamma, \quad (17)$$

where $\mathbf{\Omega}$ is a vector aligned along the direction of rotation whose magnitude is equal to the rate of rotation in radians per second. The nuclear moment precesses about the resultant field and thus departs from the true field direction. The physical picture is illustrated in Fig. 1. At $t=0$ the magnetic moment is along the original field direction. Due to the rotation, however, the magnetic moment begins to precess about the resultant field at the resonant frequency of the moment. If these conditions were maintained, this precession would continue indefinitely, and the maximum angle of a departure of the magnetic moment from the field would be 2θ where

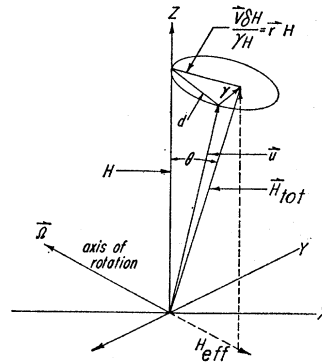


FIG. 1. Physical picture of effective field felt by a magnetic moment moving in an inhomogeneous field.

¹⁹ C. P. Slichter, *Principles of Magnetic Resonance* (Harper and Row, New York, 1963), p. 21.

θ is the angle that the total field makes with the true field.

A particle traveling in an inhomogeneous field is, in its own frame of reference, analogous to the above case. The change in the field as the particle travels can be viewed as a rotation of the field in the particle's own frame. Thus, if in the frame of the particle one transforms to a frame such that the field maintains its orientation along the z axis, one has the case shown in Fig. 1. After a collision, however, the field H_{eff} suddenly changes its directions as the flight path changes. The magnetic moment thus starts precessing about a new H_{tot} . It is this change that gives relaxation. Up to this point the discussion has been on a classical basis; but since the equations of motion of the expectation values of the quantum-mechanical operators are the same as the classical equations in this case, it is legitimate to describe problems such as the above on a classical basis and be correct quantum mechanically.

From Fig. 1 it can be seen that the displacement Δz in one flight is d/H and that

$$\Delta z = \sqrt{2}r(1 - \cos\omega\tau_c)^{1/2}, \quad (18)$$

where $\tau_c = \lambda/v$ is the gas correlation time, $\omega = \gamma H$ is the precessional frequency, and r is H_{eff}/H_0 and is the angle between H_{tot} and H_0 for small angles. One would like to find the total change in angle after n flights in terms of n and Δz .

Consider an atom in a field with a gradient just as the atom starts to make a flight after a collision. In previous flights, its magnetic moment has become disoriented from the true field direction and, as shown in Fig. 2, this disorientation can be represented by the vector \mathbf{a} in the plane of precession. The effective field is also displaced from the true field direction and its displacement is represented by the vector \mathbf{r} in Fig. 2.

During the flight the magnetic moment begins to precess as shown in Fig. 2 and eventually is displaced along the vector \mathbf{l}_2 when the next collision occurs. One wishes to find the magnitude of the vector \mathbf{b} , which is the displacement of the moment from the true field direction, in terms of $|\mathbf{a}|$ and $|\mathbf{r}|$. The angle between \mathbf{a} and \mathbf{r} is random since it is assumed that subsequent to a collision the flight direction is arbitrary.

From Fig. 2,

$$\mathbf{r} + \mathbf{l}_2 = \mathbf{b} \quad (19)$$

and

$$\mathbf{r} + \mathbf{l}_1 = \mathbf{a}. \quad (20)$$

In which case

$$\mathbf{b} = \mathbf{a} - \mathbf{l}_1 + \mathbf{l}_2 \quad (21)$$

and

$$b^2 = a^2 + l_1^2 + l_2^2 - 2\mathbf{l}_1 \cdot \mathbf{l}_2 - 2\mathbf{a} \cdot (\mathbf{l}_1 - \mathbf{l}_2). \quad (22)$$

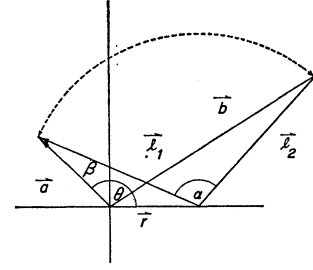
From Eq. (20),

$$\mathbf{a} \cdot \mathbf{l}_1 = \mathbf{a} \cdot \mathbf{a} - \mathbf{a} \cdot \mathbf{r}. \quad (23)$$

But when one averages over all angles between \mathbf{a} and \mathbf{r}

$$\langle \mathbf{a} \cdot \mathbf{l}_1 \rangle_{\text{av}} = a^2. \quad (24)$$

FIG. 2. Magnetic-moment displacement in a flight between collisions shown in the plane of precession.



If β is the angle between \mathbf{a} and \mathbf{l}_1 and α is $\omega\tau_c$, the precession angle in one flight, then from Fig. 2 with $|\mathbf{l}_1| = |\mathbf{l}_2|$

$$\begin{aligned} \mathbf{a} \cdot \mathbf{l}_2 &= |a| |\mathbf{l}_1| \cos(\alpha - \beta) \\ &= \mathbf{a} \cdot \mathbf{l}_1 \cos\alpha + |a| |\mathbf{l}_1| \sin\alpha \sin\beta. \end{aligned} \quad (25)$$

When one averages over all angles β , $\sin\beta \rightarrow 0$ so that

$$\mathbf{a} \cdot (\mathbf{l}_1 - \mathbf{l}_2) = a^2(1 - \cos\alpha). \quad (26)$$

From Eq. (20), after averaging over $\mathbf{r} \cdot \mathbf{a}$

$$\langle l_1^2 \rangle_{\text{av}} = a^2 + r^2. \quad (27)$$

Thus finally

$$\begin{aligned} \langle b^2 \rangle_{\text{av}} &= a^2 + 2(a^2 + r^2)(1 - \cos\alpha) - 2a^2(1 - \cos\alpha) \\ &= a^2 + 2r^2(1 - \cos\alpha). \end{aligned} \quad (28)$$

The increase in $\langle b^2 \rangle_{\text{av}}$ is just the step $(\Delta z)^2$ in one flight. Since \mathbf{a} was arbitrary, it can be seen that the mean-square deviation from the field direction in a succession of flights is just the sum of the squares of the individual steps. After n flights the angular deviation from the field is

$$\theta = \sqrt{n \langle \Delta z^2 \rangle_{\text{av}}^{1/2}}. \quad (29)$$

A suitable criterion for relaxation would be when the original expectation value of μ_z has decayed to $1/e$ th of its initial value. For $\cos\theta = 1/e$, θ is 1.19 rad, so that

$$n = 1.42 / \langle \Delta z^2 \rangle_{\text{av}}. \quad (30)$$

The number of collisions per second n' is given by v/λ and the time to decay is given by

$$T = n/n' = (1.42\lambda)/(v \langle \Delta z^2 \rangle_{\text{av}}). \quad (31)$$

One must now compute $\langle \Delta z^2 \rangle_{\text{av}}$. If a particle travels through a point $r=0$ in a field with a gradient, the rate of change in its own frame of reference is given by

$$v\delta H = \sum_i (\nabla H_i \cdot \mathbf{v}) \tilde{x}_i, \quad (32)$$

where \mathbf{a} is the displacement from the origin. If $(v\delta H/H) \ll \omega$, the rate of angular change in H is given by

$$\frac{d\theta^2}{dt} = \frac{(\nabla H_1 \cdot \mathbf{v})^2 + (\nabla H_2 \cdot \mathbf{v})^2}{H^2}. \quad (33)$$

The average of this quantity over all directions of the

vector \mathbf{v} is

$$\left\langle \frac{d\theta^2}{dt} \right\rangle_{av} = \frac{v^2}{3} \sum_m (\partial H_1 / \partial x_m)^2 + (\partial H_2 / \partial x_m)^2. \quad (34)$$

This rotation of the vector \mathbf{H} corresponds to a rate of rotation about some axis. Calling this axis Ω where $|\Omega|$ is equal to $(d\theta^2/dt)^{1/2}$, if one goes into a frame of reference rotating with \mathbf{H} along the z axis then one has as the H_{eff} of Eq. (17)

$$H_{\text{eff}} = \langle d\theta^2/dt \rangle_{av}^{1/2} / H\gamma = (v\delta H / H\gamma). \quad (35)$$

One wishes to compute $\langle \Delta z^2 \rangle_{av}$ over the probability distribution of mean free paths. This is, where the factor $(1 - \cos \omega x/v)$ comes from Eq. (18),

$$\begin{aligned} \langle \Delta z^2 \rangle_{av} &= (\delta H v / \gamma H^2)^2 \int_0^\infty \frac{2}{\lambda} e^{-x/\lambda} \left(1 - \cos \left(\frac{\omega x}{v} \right) \right) dx \\ &= (\delta H v / \gamma H^2)^2 2\omega^2 \tau_c^2 / (1 + \omega^2 \tau_c^2). \end{aligned} \quad (36)$$

In which case the relaxation time for inhomogeneous fields decay is

$$\begin{aligned} T_1 &= 2.13 \frac{(1 + \omega^2 \tau_c^2)}{\lambda v} \\ &\quad \times \frac{H^2}{\sum_m [(\partial H_1 / \partial x_m)^2 + (\partial H_2 / \partial x_m)^2]}. \end{aligned} \quad (37)$$

In the sum in the denominator, the subscripts 1 and 2 refer to the x and y direction where z is chosen at each point as the field direction. Thus in computing $(\delta H)^2$ one considers the change in field at each point perpendicular to the original field direction at each point. For example, consider the field from a point pole. There is no change in the x or y components of the field in the r direction. For a displacement at any angle, however, the change in field is

$$\partial H / r \partial \theta = H / r. \quad (38)$$

Since either angle would contribute, then

$$\sum_m (\partial H_1 / \partial x_m)^2 + (\partial H_2 / \partial x_m)^2 = 2H^2 / r^2. \quad (39)$$

EXPERIMENTAL PROCEDURES

Nuclear-Magnetic-Resonance Equipment

Most of the experiments of this paper involve the measurement of the polarization of He^3 at varying levels and gas densities. These measurements are performed in a magnetic field created by a 10-in. i.d. solenoid which is double end wound and of sixth-order design as described by Garrett.²⁰ When properly adjusted, the field of the solenoid is homogeneous to 0.23×10^{-3} G in a field of 93 G over a cylindrical sample

of 4-cm diameter by 4-cm length. Measurements of this homogeneity are made by introducing a small longitudinal magnetic field oscillating at 60 cps over the sample being tested and observing the sidebands which result from this field. If the distance from the center of the sideband line is d_1 and the half width of the signal line is d_2 and if ω is the perturbing field frequency, then

$$\Delta H = (d_1/d_2)(\omega/\gamma). \quad (40)$$

Homogeneity measurements are made on the basis of this formula.

The magnetic field must be homogeneous in time as well as in space. In order to accomplish this function the field is fed from a power supply which is current-fed back from a 1 Ω , series water-cooled resistor. The error signal from the resistor is amplified by a chopper stabilized Kintel Model 111BF amplifier with an open loop zero frequency gain of greater than 10^8 . A special filter at 60 cps feeds the input of the Kintel directly. Regulation is achieved by a series of six water-cooled power transistors in series with the solenoid. For especially fine work the magnetic-field supply must be additionally compensated in time. In order to accomplish this function a signal from a winding around the solenoid which reacts to any change is fed through a Dicke galvanometer amplifier,²¹ integrated and fed back through the pickup coil

Figure 3 shows a block diagram of the nuclear-magnetic-resonance (nmr) rig. The crystal controlled oscillator operates at 100 kc/sec and is stepped up through two frequency doublers to 400 kc/sec. Stability of frequency is important to prevent noise in the frequency-sensitive bridge circuit. The output of the oscillator system is fed through a phase shifter and amplitude control into the bridge circuit which is a resistive capacitive twin-T system. The output of the bridge is fed into a PCC 88 tuned preamplifier. The PCC 88 is a triode of unusually good noise characteristics primarily due to excellent cathode construction. By tube selection one can have an equivalent input noise resistance of as low as 5 K Ω even in the low audio range.

In the operation of the nmr equipment, in order to display a resonance, the magnetic field is varied by a

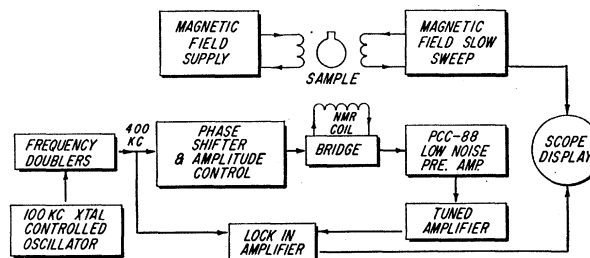


FIG. 3. Block diagram of nuclear-magnetic-resonance rig.

²⁰ M. W. Garrett, J. Appl. Phys. **22**, 1091 (1951).

²¹ R. H. Dicke, Rev. Sci. Instr. **19**, 553 (1948).

set of Helmholtz coils connected to a linear sweep circuit. The field change in one sweep can be made as large as 0.2 G or as small as 2 mG. The sweep-circuit output is also used to synchronously sweep the horizontal plates of an oscilloscope. The output of the bridge circuit, after amplification, is phase and amplitude compared with the oscillator output in a lock-in amplifier and displayed upon the vertical plates of the oscilloscope. The sensitivity of the equipment is such that the proton resonance of a ten-amagat cylindrical sample of propane gas of dimension 4 by 4 cm can be readily observed in a 93-G field. The system is designed to be barely capable of displaying the He³ resonance of a 3.1-amagat sample at equilibrium in a 123-G field. The system of sweeping the field is fast passage as described by Bloch.²² When testing a sample for polarization, the sweep rate and rotating rf field strengths are such that, generally, considerably less than a 90° pulse occurs. Because of the method of measurement, however, each test for the degree of polarization does destroy some of the alignment. When measuring a rise of polarization or a decay rate, one must compensate for the polarization disturbance arising from the act of measurement. In order to accomplish this, a previously polarized sample is placed in the nmr rig for measurement and subjected to a series of sweeps at intervals of a few seconds. The rate of depolarization due to the pulsing can then be determined from a semilog plot of the polarization versus the number of pulses. If it is assumed that each pulse destroys a γ th of the existing polarization and if $\Delta = 1 - \gamma$, then if E_0 is an initial response, $\Delta^n E_0$ is the polarization response after n pulses. A straight-line fit is made of the above plot and the ratio of the final polarization is taken to the initial value. If m is the number of pulses that have occurred on the ordinate then

$$\Delta = (E_f/E_i)^{1/m}. \quad (41)$$

When taking a series of measurements at intervals of time, a , to determine the relaxation of a sample, if initial polarization response is E_0 , the second will be $(\Delta E_0)e^{-a/T}$, and the n th would be $\Delta^n E_0 e^{-na/T}$. If one wishes to remove the effects of measurement, the procedure is merely to divide the $(n+1)$ th measurement by Δ^n .

The case of a polarization rise is somewhat more complex. Assuming that a sample initially polarized to n_0 is placed in a strong field so that it begins to change to a new value, then the polarization at any time t is given by

$$n = C(1 - e^{-t/T_1}) + n_0 e^{-t/T_1}. \quad (42)$$

The quantity C is a constant determining the ultimate polarization level. The method of computing the disturbance to the rise of the signal by the act of measurement is illustrated below for an initially unpolarized

sample tested at intervals of " a " units of time. ($T_1 = \tau$).

$$t = na \\ n_{na} = C(1 - e^{-a/\tau})(1 + \Delta e^{-a/\tau}(1 + \Delta e^{-a/\tau} \\ \times (1 + \Delta e^{-a/\tau}(\dots(1 + \Delta e^{-a/\tau})))) \dots). \quad (43)$$

The above series are summable and one has

$$n_{na} = C \frac{(1 - e^{-a/\tau})(1 - (\Delta e^{-a/\tau})^n)}{1 - \Delta e^{-a/\tau}}. \quad (44)$$

But since $t = an$, then

$$e^{-t/\tau} = (1 - K/n)/\Delta^n. \quad (45)$$

Thus in a determination of the time constant of rise, one calculates the ratio of the value to the ultimate rise, and subtracts this quantity from unity. The resulting value, if for the n th measurement, is divided by Δ^n and the data plotted on semilog paper. The above methods are at least as convenient as the more customary graphical procedures and allow irregular pulsing in decay-time measurements.

There is a considerable advantage to using a relatively low field with external enhancement for gases from the standpoint of noise. Electronics for the system can be more readily constructed with conventional components, so that the system design problem is considerably lessened. The absolute field inhomogeneity tends to be proportional to the static field and thus is considerably lessened at lower H_0 . Since ultimately the signal-to-noise ratio is proportional to the square root of T_2^* one has considerably greater sensitivity at lower fields.

The absolute polarization achieved by any particular method is derivable from the observed output signal by means of comparison to a sample of water of comparable dimension, provided the sweep causes much less than a 90° pulse. At constant frequency, number of particles, and resonance signal power, the thermal output from a He³ atom is 0.580 that of a proton. If R is the response of the proton sample and n and n' are the number of atoms per cm³ for the protons and for the He³, respectively, then the response of the He³ at equilibrium with the 123-G field is given by

$$R_T' = (0.58n'R/n). \quad (46)$$

The enhancement is given by, if R' is the measured response,

$$E = R'/R_T' = (R'n)/(0.58Rn'). \quad (47)$$

This value times the room-temperature polarization of He³ gives the absolute polarization which is achieved in any particular experiment. As a check upon the method of comparison with protons, a He³ sample can be externally enhanced to a known value in a known strong field. This enhancement can also be calculated from a comparison with protons. In a 9-kG field the enhancement is 73, and the value calculated from proton com-

²² F. Bloch, Phys. Rev. 70, 460 (1946).

parison is 68. In spite of this result, it is doubtful that polarization measurements are more than 10–20% accurate, especially when signal levels are not high.

Sample Preparation

High purity samples of He³ are prepared in a high vacuum system which is bakeable at up to 450°C under an enclosing oven. A three-stage CEC diffusion pump number CF 25 provides low-pressure capability and is used with a mechanical fore pump. The system can regularly achieve base pressures of 10⁻⁸ mm of mercury after a 350° bakeout. A copper foil trap prevents back-streaming from the diffusion pump, and a cold trap before the pump is also provided for use during filling operations. The final cleaning of He³ is provided by a charcoal trap which is baked out with the vacuum system and cooled to liquid-nitrogen temperatures prior to filling operations. He³ is handled in and given a preliminary cleaning in a separate nonbakeable system. In this system, a bakeable charcoal trap can be activated by a separate diffusion and fore pump system, and the He³ can be cycled through this trap when cooled by liquid nitrogen.

In spite of all precautions concerning cleaning and the low base pressure of the high vacuum system, samples prepared directly still show impurity spectral lines and relatively short T_1 . When, however, prior to filling, one attaches high-voltage rf electrodes (600 V_{PK} at 15 Mc/sec) to the samples to be filled, a discharge will be struck in the samples, in spite of the fact that the initial system pressure is less than 10⁻⁷ mm. An intense blue discharge appears and the system pressure rises by about four orders of magnitude. Subsequent pumping with the discharge on causes a system reduction of pressure to the 10⁻⁷-mm range while the discharge pales and ultimately disappears. If low-pressure He³ is then admitted a pure spectrum results. If, however, high-pressure He is admitted and withdrawn, faint impurity lines are observed in the resulting low-pressure sample. It was by use of a discharge that a sample having a relaxation time of 2.3×10^4 sec or 6.5 h was prepared, for it is believed that impurities become adsorbed upon a surface of either glass, quartz, or Dri Film and that the bonding is so tight that normal bakeouts cannot remove them. A gas discharge causes sufficient electron bombardment of high enough energy so that these impurities are removed from the wall, and can be evacuated by normal pumping. When the walls in this condition receive new gas, they selectively adsorb out impurities which remain when the gas is removed. If it were true that He³ forms a two-dimensional, liquid-like monolayer on a surface, then it would be reasonable to suppose that impurities would be considerably more effective in relaxation than in a bulk gas. The molecules in the gas would interchange with those on the wall.

Rubidium, mercury, wax, activated uranium, and

sodium can all be admitted into samples by means of the small, separately made vials. These vials can be held in a side tube during bakeout and discharging and their contents introduced by means of a breakoff seal. The results for T_1 when different substances are introduced into a bulb are perhaps best illustrated by Table I.

TABLE I. T_1 for various samples of He³ and foreign substances.

| Wall material | He ³ density amagats | Temp. (°C) | Foreign material in bulb | T_1 sec |
|---------------|---------------------------------|------------|--------------------------------------|-------------------|
| Pyrex | 3.1 | 295 | None | 1.2×10^3 |
| Dri Film | 3.1 | 295 | None | 1.1×10^3 |
| on Pyrex | | | | |
| Pyrex | 3.1 | 295 | None | 2.3×10^4 |
| Pyrex | 3.1 | 295 | Tungsten electrode | 1.2×10^3 |
| Quartz | 3.1 | 295 | None | 2.4×10^3 |
| Pyrex | 3.1 | 295 | Activated uranium | 6.0×10^2 |
| Pyrex | 3.1 | 295 | Rb | 10^3 |
| Pyrex | 3.1 | 295 | Rb + C ₂₀ H ₄₂ | 9.6×10^3 |
| Pyrex | 3.1 | 295 | Mercury | 3×10^3 |
| Pyrex | 3.1 | 295 | C ₂₀ H ₄₂ | 5.9×10^3 |
| Dri Film | 3.1 | 295 | Rb | 10^3 |
| on Pyrex | | | | |
| Pyrex | 1.30×10^{-3} | 295 | None | 3.9×10^3 |

Dri Film seems to have little effect on He³ relaxation, but prevents a cleaning up of the Rb vapor in Rb optical pumping. Without Dri Film it is difficult to achieve sufficient Rb pressure in a bulb without excessive temperatures.

There seem to be no definite conclusions to be shown from the table except that relaxation seems to be moderately independent of wall material. On the other hand, a Pyrex sample in which Rb has been introduced, and which was subsequently heated until the wall adsorbed the Rb and turned brown, exhibited an extremely short (less than 25 sec) relaxation time. The wall was presumably imbedded with a large number of rubidium sites which were magnetically active. Perhaps impurities form similar sites and cause relaxation. The result with mercury in a bulb of a 3×10^3 -sec time constant is the basis of the prediction that metastable pumping with mercury compression would be successful. Approximately 2 cm² free mercury surface was in the bulb.

Rubidium Optical Pumping

Figure 4 illustrates the equipment used for optical pumping of rubidium. The lamp is a 15-Mc/sec rf oscillator capable of about 20-W output coupled magnetically to a bulb approximately 3 cm in diameter containing 1-Torr neon or argon and metallic rubidium.

Air-stream cooling is used to maintain an optimum bulb temperature for maximum light output. The resonance radiation from the lamp is focused into a parallel beam which is transmitted through a Spectralab No. 2637 filter which removes the D_2 resonance line.

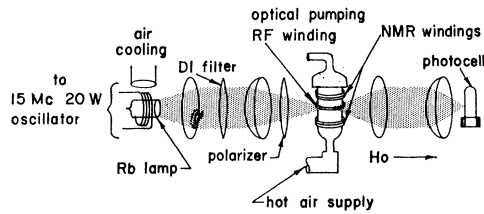


FIG. 4. Line diagram of the Rb-He³ optical pumping equipment.

Subsequently the light is focused onto the sample bulb, but between this bulb and the lens is a polaroid linear polarizer and a birefringent quarter wave plate for circular polarization. The light is collected after the sample bulb and refocused on a photocell which can monitor the light transmission.

A number of authors have discussed optical pumping^{23,24,25} as a means of imparting angular momentum to a gas. Using the methods of Franzen and Emslie, one can optically pump a gas in spite of the fact that collisions with the buffer gas can cause the hyperfine levels of the excited states of the rubidium to suffer almost complete mixing. Because the higher angular-momentum level transition of the fine structure of the resonance line is filtered out, one state of the ground-state hyperfine structure has zero probability for an optical transition. There is no state in the P level with higher angular momentum than this ground-state level so that no transition can occur because a unit of angular momentum must be absorbed. One level in the ground state thus becomes highly populated. The essential result of shining circularly polarized D_1 resonance radiation upon a sample of rubidium gas mixed with some buffer in a magnetic field is that the illuminated Rb vapor becomes polarized along or in opposition to the field. As has been discussed, it is this orientation of the Rb vapor operating through an Overhauser coupling which leads to polarization of the He³ buffer gas. The optical pumping can be monitored independently of the nuclear polarization of the He³. The hyperfine ground-state transitions in a field of about 70 G for Rb⁸⁷ exhibit splitting of 60 to 70 Mc/sec. If a magnetic field at this latter frequency is provided in the region of the sample cell, transitions can be made to occur between the various hyperfine levels of the Rb ground state at a definite value of external field. In optical pumping the selective population of the nonabsorbing state leads to a more transparent gas, but the mixing induced by the rf field results in some depopulation of the nonabsorbing state and a decrease in light transmission. In the system of this paper the steady H_0 field has a sixty-cycle component impressed upon it which causes the magnetic field to be swept back and forth through one of the hyperfine resonances. Figure 5 shows the results for the

Rb⁸⁷ $F=2$ levels. The large signal is the $F=2, 2 \rightarrow 2, 1$ transition and the smaller peaks the $F=2, 1 \rightarrow 2, 0$, $F=2, 0 \rightarrow 2, -1$, and $F=2, -1 \rightarrow 2, -2$ transitions.

The energy levels of a rubidium atom in a moderately strong magnetic field are given by the Breit-Rabi formula as

$$\lambda_{F,m_F} = \frac{1}{2} \left[\frac{A}{2} [2F-1] + \frac{Hm_F}{F} [\gamma_n(2F-1) + \gamma_e] + \frac{H^2(\gamma_n - \gamma_e)^2}{2AF} \left[1 - \frac{m_F^2}{F^2} \right] \right], \quad (48)$$

where A is a constant proportional to the nuclear-electronic coupling, γ_e and γ_n are the γ factors for the electron and nucleus, respectively, and H is the external field strength. The formula is shown for the ground state with higher total angular momentum. It is of interest to compute the differences of this formula for Rb⁸⁷ which are, with α and β constants:

$$\begin{aligned} \lambda_{2,2} - \lambda_{2,1} &= H\beta - (3/4)\alpha H^2, \\ \lambda_{2,1} - \lambda_{2,0} &= H\beta - (1/4)\alpha H^2, \\ \lambda_{2,0} - \lambda_{2,-1} &= H\beta + (1/4)\alpha H^2, \\ \lambda_{2,-1} - \lambda_{2,-2} &= H\beta + (3/4)\alpha H^2. \end{aligned} \quad (49)$$

Thus, the energy of the $2, -2 \rightarrow 2, -1$ transition is higher than that of the others. If, for a variable field

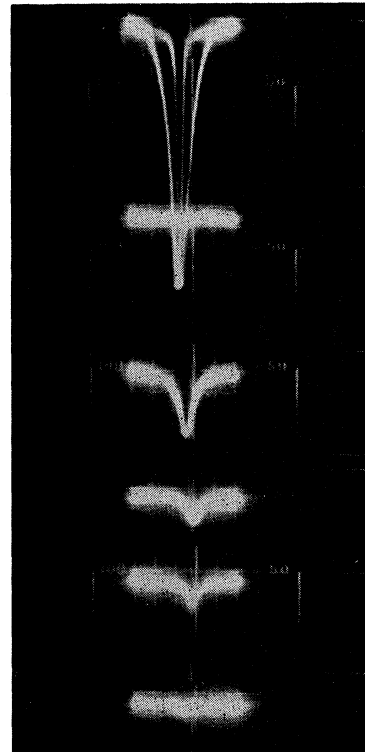


FIG. 5. Relative signal strength of light transmittance for Rb⁸⁷ $F=2$ hyperfine resonances.

²³ W. B. Hawkins and R. H. Dicke, Phys. Rev. **91**, 1008 (1953).

²⁴ J. Brossel, A. Kastler, and J. Winter, J. Phys. Radium **13**, 668 (1952).

²⁵ W. Franzen and A. G. Emslie, Phys. Rev. **108**, 1453 (1957).

but a fixed frequency, one is pumping into the $F=2, -2$ state, the largest peak will occur at the lowest field value. Conversely, if one is pumping into the $F=2, 2$ state the largest peak will be at the highest field.

From formulas (15) above, it can be seen that preferential pumping into the $2, -2$ level will result in alignment of the magnetic moments of the He^3 nuclei along the field, and an NMR signal will show absorption if $\mathbf{I}\cdot\mathbf{S}$ or scalar coupling occurs. This latter fact occurs experimentally so that one concludes that scalar coupling exists between the Rb electron and the He^3 nucleus. Absorption as opposed to emission for the He^3 system is readily observable. For a proper phase adjustment at the output of the 400-kc/sec oscillator, an emission signal is inverted from an absorption signal on the scope display. Which, is easily determined by measuring the polarization of a high field enhanced sample which must be in absorption.

No attempt will be made to determine the relative populations of the various hyperfine states of the Rb atom. It is roughly true that photon absorption from the light will be proportional to the difference in populations between the two levels tested; thus the $F2, 2$ to $F2, 1$ transition is much greater than the others and the $F2, 2$ level will be high populated. The assumption will be made on the basis of photographs such as the one shown in Fig. 5, that the $F=2, 2$ or $F=2, -2$ levels contain roughly all the particles. The photographs have this form for the region of Fig. 6 between 60 and 70°C. Figure 6 is the temperature dependence of optical pumping and nuclear polarization.

In Fig. 6, a best fit to the rise of the optical-pumping signal is made by shifting the Rb theoretical vapor-pressure curve about 10°C to the right. The curve shown is for this 10°C shift. The assumption is that for low Rb densities the optical-pumping signal is proportional to the Rb vapor pressure. Any uncertainty in the Rb vapor pressure will be reflected in the He^3 -Rb cross section result computed below. An error could easily be a factor of 2, but is probably considerably

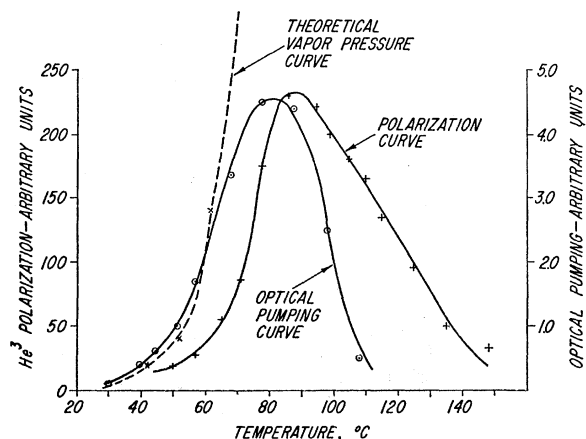


FIG. 6. Optical-pumping signal, He^3 polarization, and Rb vapor pressure as functions of temperature.

less than a factor of 10 since such a result would be some 20°C error in the Rb vapor-pressure curve. This consideration is especially true for the relatively high pressures used in these experiments.

From Eq. (16) the cross section for He^3 -Rb collision is

$$\sigma = 2n / (n_0 N \tau v). \quad (50)$$

From Fig. 6 the NMR signal at 62°C is 48. Since this curve was obtained for one e -folding time, the ultimate polarization is 71.6. This compares to a proton signal of 450 mV. The enhancement can then be computed from formula (47) and is 168 which gives n/n_0 as 1.40×10^{-5} . The velocity is 1.4×10^5 and τ is 900 sec. At a Rb vapor pressure of 2.4×10^{-6} mm Hg, which corresponds to a temperature of 52°C in the table of Scott,²⁶ N is 8.6×10^{10} . The experimental cross section is thus 1.20×10^{-24} cm². The agreement with the calculated value is reasonable. Even though a natural mixture of Rb which includes some 72% Rb^{85} of $I=5/2$ was used in experimental work, it can be readily seen that none of the above arguments concerning the cross section or type of coupling is changed. If fact, the natural mixture of two isotopes aids in pumping at higher pressures. Because of isotope shift, useful spectral emission is large and self-reversal problems are lessened.

Inhomogeneous Fields Relaxation

If a sample of He^3 which has been previously polarized is placed in the field of a bar magnet which is large compared to that of the earth's field, and if $\omega\tau_c \ll 1$, then from Eqs. (37) and (39)

$$T_1 = (2.13r^2/2\lambda v). \quad (51)$$

An experiment was performed in which polarized samples of He^3 at densities of 3.5, 2.6, and 1.6 amagats were held in a point pole field at distances of 5, 12, and 8 cm. The point pole field was 80 G at 2 cm so that it dominated the earth's field over the range of measurement. The samples were held in the point pole field for a measured period of time, removed and tested for polarization and inserted again and measured until the polarization signal sank into noise. The measured and calculated values are shown in Table II. The agreement is close. All samples had relaxation times in homogeneous fields of greater than 10^3 sec.

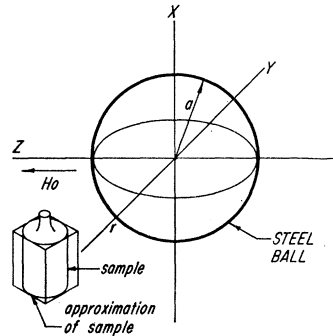
A measurement was also undertaken to determine the

TABLE II. Relaxation of He^3 in the field of a bar magnet.

| $H^2/(\delta H)^2$ Density amagats | 12.5 | | 32 | | 72 | |
|--|-------|------|-------|------|-------|------|
| | Calc. | Exp. | Calc. | Exp. | Calc. | Exp. |
| 3.1 | 20.4 | 20.5 | 52.2 | 51.0 | 117 | 90 |
| 2.5 | | | 42.0 | 39.0 | | |
| 1.6 | | | 27.0 | 26.0 | | |

²⁶ D. H. Scott, Phil. Mag. 47, 32 (1924).

FIG. 7. The experimental arrangement for the measurement of rise time of polarization in an inhomogeneous magnetic field.



rise time and extent of polarization in a field of given inhomogeneity. A 2-cm-radius spherical ball of Armco magnet iron was placed in the field of a Varian magnet at 6000 G. At this level of field the relative permeability of the iron is much greater than one. The magnetic scalar potential external to the ball is given by

$$\phi = H_0[(a^3 \cos\theta/r^2) - r \cos\theta], \quad (52)$$

where a is the radius of the ball and H_0 is the external field value, and the polar axis is along the direction of the external field.

If a sample of gas is placed in the x - y plane of the field of the ball, only an atom moving along the polar axis will see a change in the direction of field. Since

$$\frac{\partial H_x}{\partial z} = \frac{H_0 3xa^3}{r^5}; \quad \frac{\partial H_y}{\partial z} = \frac{H_0 3ya^3}{r^5}. \quad (53)$$

If it is assumed that $a/r \ll 1$ then

$$\frac{H^2}{\sum_m (\partial H_x / \partial x_m)^2 + (\partial H_y / \partial x_m)^2} = \frac{r^8}{9a^6}. \quad (54)$$

The experimental arrangement is shown in Fig. 7. A sample of gas is held at a certain distance from the steel ball for a definite period of time. The resulting polarization is then measured and the sample returned to the magnet for another period. The samples tested all had relaxation times of greater than 10^3 sec in homogeneous fields. Since a sample in the field of the ball extends over a distance relatively large compared to the dimensions of the ball, one must average the relaxation rates over the sample. If the assumption is made that the diffusion time of the He³ over the sample is short compared to the relaxation time then a suitable average is

$$\langle 1/T_1 \rangle_{av} = \int (1/T_1) dv / \int dv. \quad (55)$$

This integral is approximated by considering the r dependence only so that the shape of the sample is considered to be a small solid spherical section as shown in Fig. 7. If b is the distance of the sample at its closest

point and c is its most distant point then

$$\left\langle \frac{1}{T_1} \right\rangle_{av} = \frac{27a^6(b^{-5} - c^{-5})}{10(c^3 - b^3)}. \quad (56)$$

Table III compares the experimental values. The

TABLE III. Calculated and experimental values for T_1 in sec dipole-field rise times for 4-cm steel ball in 6 kG Varian field.

| Density amagats | b, cm | | c, cm | | 3.0 | |
|--------------------|---------|------|---------|------|-------|------|
| | 2.0 | 2.5 | 6.0 | 6.5 | 7.0 | |
| | Calc. | Exp. | Calc. | Exp. | Calc. | Exp. |
| 3.1 | 31 | 40 | 124 | 137 | 350 | 180 |
| 2.3 | | | 92 | 95 | | |
| 1.45 | | | 58 | 62 | | |
| 0.86 | | | 34 | 37 | | |

crudity of the average of the calculated values probably leads to the discrepancies. The levels of polarization reached in these experiments were independent of the rise time. Polarization levels reached are thus those of thermal equilibrium in the average field. No measurements have been made concerning the region where $\omega\tau \gg 1$. It would be a good confirmation of the theory should formula 37 apply under such conditions.

He³-He³ Optical Pumping

Figure 8 shows a diagram of the He³-He³ optical-pumping system. The oscillator has two Eimac 4CX300A triode tubes connected in cross coupled push-pull. The total tank circuit is a single wire system which loops around a quartz button approximately 1/4-in. thick by 1 in. in diameter which contains 1/2 Torr of He⁴. In order to maintain pressure in the button, a glass reservoir is supplied through a glass-to-quartz seal. This pressure control and level is believed to contribute greatly to the brightness of the lamp at the proper wavelength and thus to the high polarizations reported below. The oscillator operates at about 100 Mc/sec. A spherical reflector focuses the light from the button onto an $f/1.5$ or $f/2$ converging lens and then through a Polaroid linear polarizer and quarter wave plate. One can maintain excellent brightness of the

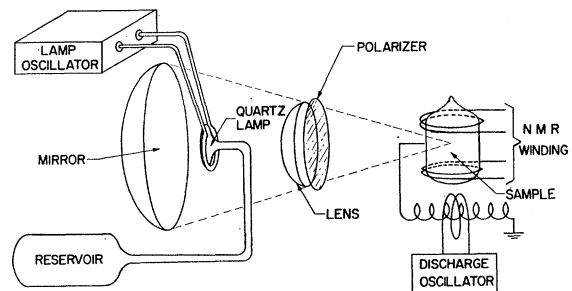


FIG. 8. Line diagram for experimental arrangement used for He³ polarization by metastable optical pumping.

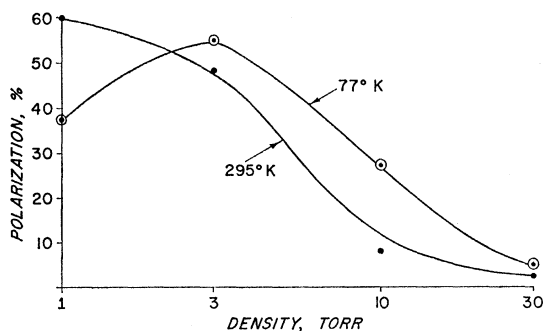


FIG. 9. Graph of polarization versus density for He^3 polarized by means of He^3 metastable optical pumping.

image on the bulb by this system. The circularly polarized light at $10\,830\text{ \AA}$ is used to illuminate a sample of He^3 in which a weak rf discharge has been struck. The rf source for this discharge is a 1.5-Mc/sec oscillator at 500 V and is current limited by the variable capacitor. In the sample it has been possible to maintain extremely weak, almost invisible, discharges. It is observed that one can pass through a maximum polarization as the discharge weakened.

The energy separating the two levels of a He^3 atom in the NMR field is νh , where ν is 400 kc/sec. The net polarization of the He^3 at room temperature is then 3.23×10^{-8} . Using Formula (47), the polarization can be computed for various conditions. Room-temperature and 77°K results are given in Fig. 9.

The optical pumping at liquid-nitrogen temperature was performed in an unsilvered Dewar flask. The NMR coils were wound over the outside of the Dewar and no particular noise problems were noted because of the bubbling of nitrogen around the samples.

The polarization experiments on metastable He^3 were light limited in the sense that a straight edge cutting out half the light would halve the polarization. In order to achieve greater polarization at higher pressures either a greater light intensity or a greater concentration of metastables would be required.

As mentioned in the introduction, the limit on the number of metastables is probably due to metastable-metastable collisions or free-electron interactions with metastables, in which case one would gain only about a factor of 2 because of lessened mobilities at 77°K . Colegrove, Walters, and Schearer²⁷ have measured the metastability exchange cross section as a function of temperature. Their results could explain the decrease of polarization with temperature at 1-mm pressure.

The relaxation time of 1-mm samples is on the order of 4×10^8 sec which is similar to T_1 for one to three-atmosphere samples. If the relaxation were proportional to the number of particles striking a wall, which would be the case if collisions with the wall were not correlated and if the diffusion time of a particle across the sample

were short compared to the relaxation time, the relaxation time would be independent of pressure. This view is apparently the case.

Motional narrowing of line width of an NMR signal due to diffusion of particles in a 1-Torr sample as described by Colegrove, Schearer, and Walters⁴ did not occur in the above work. This difference is due to greater field homogeneity and rapid sweep rates, so that any motional narrowing over the inhomogeneity was less pronounced.

Discharges at High Pressure

Samples of pure He^3 at 3.1 amagats in Pyrex with a tungsten electrode were prepared. The tungsten electrode allows for the creation of a discharge in the high-pressure gas.

When such samples are enhanced in a 10-kG field the relaxation time is of the order of 1.2×10^8 sec. If, however, a gas discharge is struck in the sample by means of the electrode and an rf source, the polarization does not tend toward the equilibrium value for the field, but to generally enhanced values with alignment of the nuclear spins either with or against the field.

If the discharge is supplied by means of a Cenco #80721 Tesla coil, the nuclei polarize in steady state to an enhanced value of about 4.4 times that of thermal equilibrium in the 10-kG field. Furthermore, the polarization is in opposition to the field. The output of the Tesla coil is on the order of 40 kV and consists of bursts of pulses of rf energy during the peak portion of the sixty-cycle period. The individual pulses in each burst are separated by a distance of about $100\text{ }\mu\text{sec}$ and individually are the ring-down of a 4-Mc/sec oscillating circuit having a Q of about 25. The rise time of the polarization measures 120 sec.

If, instead of the Tesla coil, a 1-Mc/sec steady-state oscillator is used as the source of the discharge, the polarization is again enhanced by 4.6 but the direction of alignment is with the field. The rise time of the polarization is 292 sec. These effects are undoubtedly manifestations of the Overhauser effect acting between the He^3 nuclei and some saturated product from the discharge. For example, suppose some subspecies were formed in the discharge with an electronic magnetic moment. If this species were formed in an electronic collision, it is reasonable to suppose that it would have a spin temperature on the order of 10^4 deg, or in other words, be essentially saturated. If fairly strong coupling were to exist with the He^3 nuclei, one might expect that the Overhauser effect would act as a polarization mechanism. If metastable He^3 were the subspecies, then a mechanism of polarization coupling would exist through metastability exchange and this mechanism would be such that polarization in opposition to the field would occur. Extrapolating Phelps²⁷ data on three-body destruction, one would expect a lifetime of triplet metastables of only a few microseconds. Meta-

²⁷ F. D. Colegrove, L. D. Schearer, and G. K. Walters, Phys. Rev. **135A**, 355 (1964).

stable molecules, however, could exist some time before diffusion to the walls. In an intermittent discharge one would expect a high density of triplet metastables relative to free electrons, ions, or singlet metastables. Without further knowledge, one might thus attribute the reverse enhancement observed in a high-pressure sample under intermittent discharge conditions to the formation of a high proportion of saturated metastables or metastable molecules.

Under conditions of continuous discharge, the triplet metastables population is lower according to Phelps than that subsequent to the discharge. There are also free electrons and singlet metastables in the discharge; thus if direct electronic excitation by electrons led to a preferred population of a $^1P_{3/2}$ M sublevel one would have an effect. It is perhaps most probable that enhancement in the continuous discharge case arises from a dipolar coupling to free electrons. The type of interaction would have to be dipolar or $I \pm S \pm$ and the electrons saturated. Further investigation is needed to elucidate these processes.

CONCLUSIONS

Electronic overlap effects between rubidium and He³ cause an enhancement of the scalar or hyperfine interaction between the Rb electron and He³ nucleus. As a result the interaction is strong enough to cause a polarization of the nuclei of He³ when the latter is used as a buffer gas in Rb optical pumping. The strength of the interaction is not great enough that the He³ nuclear polarization is determined by the level of Rb polarization. The time constant of decay of the He³ nuclei in a bulb is virtually independent of temperature in the measurable range of from 70 to 150°C whereas the Rb vapor pressure varies about three orders of magnitude over the same interval. When one attempts to increase the interaction between the Rb and He³ by means of increasing the Rb pressure, difficulties are encountered in Rb optical pumping. The Rb atoms become numerous enough that ground-state interactions between them begin to rob the system of its angular momentum. Experimentally, one observes the enhancement mechanism to fail above 110°C as seen in Fig. 6. One cannot control the strength of the Rb-He interaction, nor of permissible Rb pressures except that a greater light intensity would result in the ability to optically pump at higher pressures. The only other alternative would be to increase the relaxation times of the present samples which run about 10^8 sec. Perhaps wall surfaces that have no reactivity with Rb and which were cleaned to the extent of the pure samples reported in this paper would permit a gain of an order of magnitude in relaxation time. It is hard to imagine a factor of 5×10^8 coming from either an increase in light intensity or relaxation time or both. Present values of polarization are 0.01% and one needs 50% for nuclear-physics or elementary-particle work. On the other hand, polariza-

tion of 0.01% in a 3.1-atm sample is sufficient to create strong signals from reasonably sized samples. Such a system might be used in a gyroscope, in computer storage systems, or in other such devices.

Perhaps the most promising means of achieving 50% polarization in a 1- to 3-atm sample is to use He³ metastable optical pumping. As has been pointed out, the relaxation of He³ nuclear polarization over a clean mercury surface is comparable to that of Pyrex. Since the low pressures which must be used in metastable pumping limit the usefulness of a sample directly pumped, one can conclude that a process of physical compression following the achievement of polarization would be required to create a sample of 50% polarization at an atmosphere or greater. If the equilibrium polarization in a sample which is being optically pumped over its whole volume V_1 , at a pressure P_1 , is K , and if it has a time constant of rise of τ_1 , and if P_2 , V_2 , and τ_2 are the pressure, volume, and time constant of the final configuration, then for high polarization

$$V_1 \gg (P_2/P_1)(\tau_1/\tau_2)V_2. \quad (57)$$

If the pressure multiplication is 10^3 and since $\tau \approx 50$ and $\tau_2 \approx 4 \times 10^8$ then

$$V_1 \gg 12V_2. \quad (58)$$

Such a ratio could easily be obtained.

Inhomogeneous field relaxation can be used to polarize He³ to an extent greater than is possible with steady fields. Because the time constant of polarization is under the control of the experimenter, he can apply intense but highly inhomogeneous fields for a short time. Because T_1 is short, under these conditions, the sample will polarize to an appreciable extent. When the intense driving field is removed, however, if one has immersed the sample in a homogeneous field, T_1 will be long. A second short intense pulse will cause more polarization. One thus has a ratchet-like effect which will raise the degree of polarization to a level approaching the average of the intense field over a pulse. Since pulsed fields can generally be made more powerful than steady fields, a fairly easy mechanism of polarization exists to levels which are useful for all but the highest degrees of polarization. The quantity $(H/\delta H)^2$ is a function of the coordinates alone for a given type of source as is $r^2/2$ for a point pole field. In a three-amagat sample λv is on the order of 1.2 cm²/sec. Presumably a point pole field could be made on the order of half a millimeter in diameter and act over a half-millimeter region. At three amagats T_1 would be on the order of 5 msec for fields to 10^3 kG at room temperature. In general, the greatest field permitted before $\omega\tau_e$ becomes greater than one so that T_1 begins to lengthen as H^2 is

$$H_{\max} = v/(\gamma\lambda). \quad (59)$$

One must of course average T over a ratcheting volume, and limit this volume to a high-field region.

At present, high-pressure discharge polarization is

more an interesting example of the Overhauser effect than a useful mechanism for obtaining magnetized He³. Future work might show how one could achieve polarization approaching electronic levels. In this case, easily reachable fields and temperatures might result in high degrees of polarization.

In work associated with nuclear magnetism at moderate pressures in gases, the relaxation time tends to be long enough that considerable care must be exercised in preventing inhomogeneous field relaxation from dominating the decay mechanism. It is simply not true that a simple Helmholtz pair will allow sufficient homogeneity to prevent relaxation times in 1-Torr samples from being on the order of seconds. The relaxation time of a Torr sample in a field which rotates some 3° in a centimeter will be on the order of 10 sec which will be some 400 times shorter than its natural relaxation time.

The enhancement mechanism in Rb-He³ interactions appears to arise strictly from the overlap of the electrons

of the He³ atom and the Rb valence electron. It is interesting that such a simple model can account for the observed cross section. The availability of an easy means of finding atomic orbitals from Herman and Skillman's²⁸ computer program should allow the implications of overlap effects for alkali-noble gas nuclear-electronic interactions to be explored.

ACKNOWLEDGMENTS

Clark Varnum worked on the problem of rubidium optical pumping as a mechanism for He³ polarization until his death in 1961. The authors wish to express their appreciation for the use of much of his excellently designed equipment and his carefully prepared records.

This work was supported by the National Science Foundation and their assistance is gratefully acknowledged.

²⁸ F. Herman and S. Skillman, *Atomic Structure Calculations* (Prentice-Hall, Inc., Englewood Cliffs, New Jersey, 1963).

Generation of Stokes and Anti-Stokes Radiation in Raman Media

H. A. HAUS

Department of Electrical Engineering and the Research Laboratory of Electronics, Massachusetts Institute of Technology, Cambridge, Massachusetts

AND

P. L. KELLEY AND H. J. ZEIGER

Lincoln Laboratory, Massachusetts Institute of Technology, Lexington, Massachusetts*

(Received 11 August 1964; revised manuscript received 8 January 1965)

A three-dimensional analysis of stimulated Raman emission is presented for a medium through which a cylindrical laser beam passes. The buildup of the Stokes radiation from the spontaneous fluctuations in the Raman medium is considered. A generalization of the fluctuation-dissipation theorem is derived relating the current-current fluctuations at the Stokes frequency to the laser-induced (negative) conductance at this frequency. The anti-Stokes radiation is treated as arising from the interaction of the laser field and the molecular vibrations accompanying the Stokes radiation. The anti-Stokes radiation emerges in a narrow cone around the familiar phase-matching direction given by $\beta_- = 2\mathbf{k}_L - \beta_+$, where β_- and β_+ are the (real parts of the) propagation constants of Stokes and anti-Stokes waves in the medium, and \mathbf{k}_L is the laser propagation vector. The angular width of the anti-Stokes radiation cone is evaluated.

I. INTRODUCTION

FOLLOWING the first observation of stimulated Stokes emission in a cavity structure,¹ Terhune² and co-workers reported the observation of anti-Stokes radiation emitted in rings when a Q-switched ruby laser was focused on a Raman scattering medium. Garmire *et al.*,³ and Chiao *et al.*⁴ discussed a number of

phenomena involving the coherent production of Stokes and anti-Stokes radiation, based on a macroscopic plane-wave treatment of the coupled equations describing the emission processes. This model leads to the prediction that a phase-matched condition occurs in which plane Stokes and anti-Stokes waves are strongly coupled; when this occurs they will suppress each other, giving no exponential growth of either Stokes or anti-Stokes radiation for the phase-matched waves. Hellwarth⁵ examined the equations for the case of temporal rather than spatial growth. Bloembergen and Shen⁶ found that

* Operated with support from the U. S. Air Force.
¹ G. Eckhardt, R. W. Hellwarth, F. J. McClung, S. E. Schwarz, D. Weiner, and E. J. Woodbury, *Phys. Rev. Letters* **9**, 455 (1962).
² R. W. Terhune, *Bull. Am. Phys. Soc.* **8**, 359 (1963).
³ E. Garmire, F. Pandarese, and C. H. Townes, *Phys. Rev. Letters* **11**, 160 (1963).
⁴ R. Y. Chiao, E. Garmire, and C. H. Townes (to be published).

⁵ R. W. Hellwarth, *Current Sci. (India)* **33**, 129 (1964).

⁶ N. Bloembergen and R. Shen, *Phys. Rev. Letters* **12**, 504 (1964).

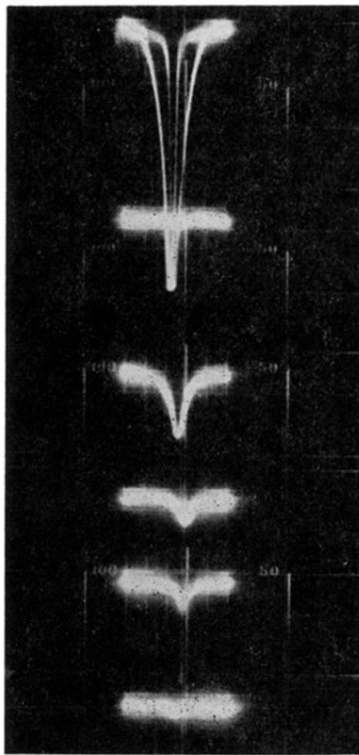


FIG. 5. Relative signal strength of light transmittance for Rb^{87} $F=2$ hyperfine resonances.